Acta Oceanol. Sin., 2024, Vol. 43, No. 6, P. 131–141
https://doi.org/10.1007/s13131-024-2376-x
http://www.aosocean.com
E-mail: ocean2@hyxb.org.cn

Effects of phosphorus limitation on sinking velocities of phytoplankton during summer in the Changjiang River Estuary

Xinchi You[1, 2, 3], Qiang Hao[3, 4], Jie Zhu[1, 3], Wei Zhang[3, 4], Haiyan Jin[2, 3, 4], Dewang Li[3, 4], Huanhong Ji[5, 6], Yu Ke[5, 6], Feng Zhou[2, 1, 7*]

[1] Ocean College, Zhejiang University, Zhoushan 316021, China

[2] State Key Laboratory of Satellite Ocean Environment Dynamics, Second Institute of Oceanography, Ministry of Natural Resources, Hangzhou 310000, China

[3] Key Laboratory of Marine Ecosystem Dynamics, Second Institute of Oceanography, Ministry of Natural Resources, Hangzhou 310012, China

[4] Donghai Laboratory, Zhoushan 316021, China

[5] East China Sea Ecological Center, Ministry of Natural Resources, Shanghai 201206, China

[6] Key Laboratory of Marine Ecological Monitoring and Restoration Technologies, Ministry of Natural Resources, Shanghai 201206, China

[7] Observation and Research Station of Yangtze River Delta Marine Ecosystems, Ministry of Natural Resources, Zhoushan 316021, China

Received 21 November 2023; accepted 2 February 2024

Abstract

The sinking of phytoplankton is critical to organic matter transportation in the ocean and it is an essential process for the formation of coastal hypoxic zones. This study was based on a field investigation conducted during the summer of 2022 in the Changjiang River (Yangtze River) Estuary (CJE) and its adjacent waters. The settling column method was employed to measure the sinking velocity (SV) of different size fractions of phytoplankton at the surface of the sea and to analyze their environmental control mechanisms. The findings reveal significant spatial variation in phytoplankton SV (–0.55–2.41 m/d) within the CJE. High-speed sinking was predominantly observed in phosphate-depleted regions beyond the CJE front. At the same time, an upward trend was more commonly observed in the phosphate-rich regions near the CJE mouth. The SV ranges for different size-fractionated phytoplankton, including micro- (>20 μm), nano- (2–20 μm), and picophytoplankton (0.7–2 μm), were –0.50–4.74 m/d, –1.04–1.59 m/d, and –1.24–1.65 m/d, respectively. Correlation analysis revealed a significant negative correlation between SV and dissolved inorganic phosphorus (DIP), implying that the influence of DIP contributes to SV. The variations in phytoplankton alkaline phosphatase activity suggested a significant increase in SV across all size fractions in the event of phosphorus limitation. Phytoplankton communities with limited photosynthetic capacity (maximum photochemical efficience, Fv/Fm < 0.3) were found to have higher SV than that of communities with strong capacity, suggesting a link between sinking and alterations in physiological conditions due to phosphate depletion. The findings from the *in situ* phosphate enrichment experiments confirmed a marked decrease in SV following phosphate supplementation. These findings suggest that phosphorus limitation is the primary driver of elevated SV in the CJE. This study enhances the comprehension of the potential mechanisms underlying hypoxic zone formation in the CJE, providing novel insights into how nearshore eutrophication influences organic carbon migration.

Key words: phytoplankton, sinking velocity, Changjiang River Estuary, phosphorus limitation, alkaline phosphatase

Citation: You Xinchi, Hao Qiang, Zhu Jie, Zhang Wei, Jin Haiyan, Li Dewang, Ji Huanhong, Ke Yu, Zhou Feng. 2024. Effects of phosphorus limitation on sinking velocities of phytoplankton during summer in the Changjiang River Estuary. Acta Oceanologica Sinica, 43(6): 131–141, doi: 10.1007/s13131-024-2376-x

1 Introduction

As organic matter accumulates in the ocean (Huisman et al., 2002), it frequently descends towards the seafloor owing to its density surpassing that of seawater (Huisman and Sommeijer, 2002). This sinking speed is commonly termed the phytoplankton sinking velocity (SV). Phytoplankton with high SV are a crucial component of the marine biological pump, facilitating the transfer of surface organic carbon to the deep sea (Falkowski,

Foundation item: The National Programme on Global Change and Air-Sea Interaction (Phase Ⅱ)—Hypoxia and Acidification Monitoring and Warning Project in the CE under contract No. GASI-01-CJK; the Science Foundation of Donghai Laboratory under contract No. DH-2022KF0215; the Oceanic Interdisciplinary Program of Shanghai Jiao Tong University and Scientific Research Fund of the Second Institute of Oceanography, MNR under contract No. SL2022ZD207; the National Key R&D Program of China under contract No. 2021YFC3101702; the Long-term Observation and Research Plan in the Changjiang Estuary and Adjacent East China Sea (LORCE) Project under contract No. SZ2001.

*Corresponding author, E-mail: zhoufeng@sio.org.cn

2002). However, when the SV is excessively low, these phytoplankton become susceptible to fragmentation and degradation, consequently diminishing their role in carbon sequestration. In the vicinity of the Changjiang River (Yangtze River) Estuary (CJE), the sinking of phytoplankton plays a significant role in hypoxic zone formation (Sun et al., 2022; Wang et al., 2017; Zhou et al., 2020, 2021).

An association between the sinking pattern of phytoplankton and their physiological state has been reported (Anderson and Sweeney, 1978; Bienfang et al., 1982; Eppley et al., 1967; Reynolds, 2006; Smayda, 1970). During the exponential growth phase, cells exhibit optimal physiological conditions and a lower SV, while the opposite is observed during the decline phase. Environmental factors, including light (Bienfang, 1984; Johnson and Smith, 1986; Petrucciani et al., 2023; Riebesell, 1989; Waite et al., 1992b; Waite, 1997), temperature (Eppley, 1972), salinity (Pilkaitytė et al., 2004), nutrients (Bach et al., 2019; Bienfang, 1981a; Bienfang and Harrison, 1984; Cloern, 2001; Eppley et al., 1967; Muggli et al., 1996; Sundareshwar et al., 2003; Waite et al., 1992a), and acidification (Cai et al., 2022) can influence the physiological state of phytoplankton, with nutrient limitation exerting the most rapid and profound effect.

Owing to the excessive nitrogen input from the Changjiang River runoff, the nitrogen-to-phosphate ratio is elevated in the CJE and its adjacent waters (N/P > 80 in general) (Yang et al., 2023; Tseng et al., 2014), particularly in the surface seawater (Liu et al., 2016), exceeding the Redfield ratio (N/P = 16) (Redfield et al., 1963). This leads to the possibility of the region experiencing a limitation in phosphate availability (Liu et al., 2016; Mo et al., 2020; Wang et al., 2013). In seawater, phosphorus exists in the form of dissolved inorganic phosphorus (DIP) or dissolved organic phosphorus, with DIP being the only form directly utilizable by organisms (Correll, 1998). In situations of scarce DIP, phytoplankton resort to decomposing dissolved organic phosphorus to access DIP through processes such as alkaline phosphatase (Hoppe, 2003) or other mechanisms (Luo et al., 2017; Zhang et al., 2020). Numerous studies have regarded the elevation of alkaline phosphatase activity (APA) (Ammerman, 1991) as a reliable indicator of phosphorus limitation in phytoplankton (Labry et al., 2005; Tseng et al., 2014). Phytoplankton obtain phosphorus through diverse mechanisms because it is an essential nutrient for their growth. Limitation in phosphorus can lead to alteration in gene expression within phytoplankton cells (Haley et al., 2017), reduce protein and RNA content (Dyhrman et al., 2012), modify amino acid composition (Grosse et al., 2017), and alter enzyme quantities (Casey et al., 2016). Bienfang et al. (1982) laboratory experiment revealed that phosphorus limitation promoted phytoplankton sinking. Moreover, Wang et al. (2022b) found that phosphorus limitation results in a 37%–44% increase in SV. Guo et al. (2016) and Li et al. (2018) conducted field investigations on phytoplankton SV in the CJE and its adjacent areas. However, they did not prioritize SV spatial distribution in their study or phosphorus limitation. The influence of phosphorus limitation on phytoplankton SV under natural conditions remains unclear.

The primary hypothesis of this study posits that phosphorus limitation facilitates phytoplankton sinking. A scientific survey was conducted during the summer of 2022 in the CJE and its adjacent waters to test this hypothesis. In addition, *in situ* phosphate enrichment experiments were performed. Therefore, this study aimed to assess the intrinsic relationship between SV and DIP concentrations by analyzing the phytoplankton sinking mechanism under conditions of phosphorus limitation, which could enhance our understanding of the potential mechanisms via which surface phytoplankton sink beneath the mixed layer.

2 Materials and methods

2.1 *Station selection and sample collection*

The field investigation for this study was conducted in the CJE and its surrounding waters from July 31 to August 6, 2022. Figure 1 depicts the station layout, encompassing 23 stations distributed across six transects. A surface water sample (0.5 m depth) was collected using a water sampler to measure chlorophyll *a* (Chl *a*), APA, SV, maximum photochemical efficiency (Fv/Fm) and to conduct *in situ* phosphate enrichment experiments. The Fv/Fm values were measured along the N, J, A, and B transects, with separate water sampling for the enrichment experiments conducted. All the measurements were performed using triplicate samples.

A conductivity-temperature-depth (CTD) sensor (SBE 911 CTD, Sea-bird Scientific, Washington, USA) was used to collect surface temperature, salinity, and turbidity data from the surveyed area. Additionally, 60 mL water samples were collected and filtered through 0.45 μm acetate fiber filters (CAT No. 70000004, Whatman, Buckinghamshire, UK) and stored frozen at –20℃ till further use. Subsequently, they were thawed in the laboratory and subjected to DIP concentration measurements using the spectrophotometric method (Grasshoff et al., 1976), employing an automated segmented flow analyzer (SmartChem® 600, AMS Alliance, Frépillon, France). In an acidic medium containing potassium antimonyl tartrate (pH < 1), the phosphates in the water samples react with ammonium molybdate to form a phosphomolybdic heteropolyacid. The latter is then reduced by ascorbic acid to produce a blue-colored complex; its absorbance is measured at a wavelength of 880 nm.

2.2 *Chl a determination*

The fluorescence extraction method was used to determine Chl *a* concentration in various size fractions. To isolate distinct phytoplankton fractions, 100 mL water samples were sequentially filtered through 20 μm, 2 μm, and Whatman GF/F glass fiber (approximately 0.7 μm) filter membranes under low vacuum pressure (≤30 kPa) during field sampling. A 20 μm nylon net (NY2002500, Merck Millipore Ltd., T45 Carrigtwohill, Ireland),

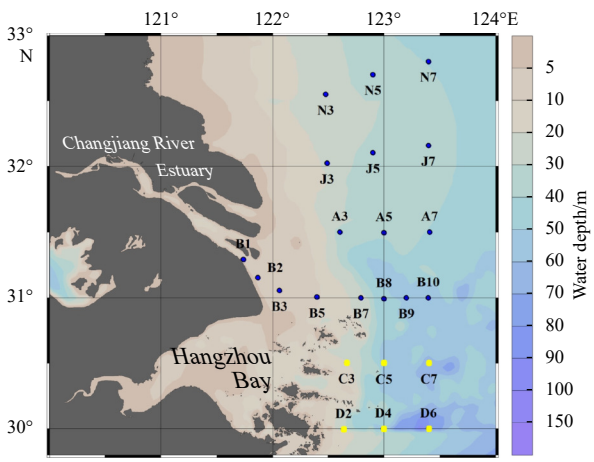

Fig. 1. Station layout. Fv/Fm was measured at the deep blue stations.

2 μm filters (unspecified model, THU, Beijing, China), and GF/F glass microfiber filters (CAT No.1825-025, Whatman, Buckinghamshire, UK) were used. These fractions were categorized into micro- (>20 μm), nano- (2–20 μm), and pico- (0.7–2 μm) sizes. All the membranes were stored at −20℃. Upon returning to the laboratory, the membranes were placed under low-light conditions and submerged in a 90% volume fraction acetone solution at −20℃ for 24 h before the extraction process. The extracted solution was subsequently analyzed at 20–25℃ using a Turner-Designs Trilogy® laboratory fluorometer. Total-Chl *a* concentration was determined by combining micro-Chl *a*, nano-Chl *a*, and pico-Chl *a* concentration. In the following discussions, the Chl *a* values for various size fractions, including the total, were expressed as absolute values, serving as the biomass metric for subsequent calculations and discussions.

2.3 *APA determination*

The p-nitrophenyl phosphate (PNP-P) technique was used to analyze the APA with various size fractions (Li et al., 1998). Water samples were filtered as described in Section 2.2 to obtain the respective fractions. Furthermore, the filtrate obtained after passing the water samples through 0.45 μm acetate fiber filters was also collected. Before analysis, the filters and filtrate were stored in the dark at −20℃. After thawing in the laboratory, the filter was immersed in 5 mL of the corresponding filtrate from the same station to create a composite sample. Subsequently, 675 μL of pH 8.2 Tris-HCl buffer and 325 μL of 10 mmol/L PNP-P solution were added to the composite and a blank filtrate. For 24 h, the reaction was conducted in a temperature-controlled water bath shaker set at 30℃, with continuous agitation at 100 r/min. Following that, the absorbance at 405 nm was swiftly measured using a UV-visible spectrophotometer (752N, INESA, Shanghai, China). Total-APA was calculated by summing the concentrations of micro-, nano-, and pico-APAs.

2.4 *Phytoplankton SV determination*

Measurements were taken using the settling column (SETCOL) method (Bienfang, 1981b). The SETCOLs used in the study were 1 m long and comprised non-transparent hollow cylinders with a total volume of 1.1 L. They contained three interconnected compartments, each fitted with valves. During the measurements, consistent seawater was injected into three SETCOLs, with the compartments remaining interconnected for 4 h. Subsequently, the valves were closed, and water samples were collected from each of the three compartments for Chl *a* analysis, as described earlier in Section 2.2, which was then used to calculate the SV as described below.

$$\mathrm{SV} = \frac{B_\mathrm{s}}{B_\mathrm{t}} \cdot \frac{L}{t}, \tag{1}$$

where B_s represents the biomass settled into the bottom compartment; B_t denotes the total biomass; L signifies the length of the space inside the SETCOL; and t indicates the sinking duration.

2.5 *In situ phosphate enrichment experiments*

Water samples were collected from stations B8 (31.00°N, 123.00°E) and N6 (32.76°N, 123.17°E) for the *in situ* phosphate enrichment experiments. At each station, 40 L of surface seawater was collected and subsequently divided equally into four transparent containers. Two of these containers were designated as the enrichment group, while the remaining two were considered as the control group. The DIP concentration was augmented by 10 μmol/L in the two enrichment experimental groups by adding NaH_2PO_4 solution [XBML-M1 f/2 medium kits (1000x) (NaH_2PO_4), Pulan Biological Science and Technology Co., Ltd., Xiamen, China]. Subsequently, all the four containers were placed in a culture chamber on the deck and cultivated for 24 h. To replicate the light intensity observed in the mixed layer, the culture chamber was positioned in direct sunlight and shielded with a semi-transparent membrane. Additionally, to simulate sea surface temperature, surface seawater was added to the culture chamber. The SV was measured after incubation. Based on the method described in Section 2.4, since three parallel samples were obtained for each container for SV measurement, resulting in six parallel samples for both the enrichment and control groups at each station .

2.6 *Fv/Fm determination*

In situ Fv/Fm measurements were taken at 17 stations located on N, J, A, and B transects (depicted as the deep blue sites in Fig. 1). Before measuring, a 10 mL sample of surface seawater was collected. Furthermore, another 10 mL surface seawater was filtered through a 0.45 μm acetate fiber membrane to generate a filtrate for background determination. The optimal photochemical efficiency of the sample was determined using water pulse amplitude-modulated fluorometry (Heinz Walz GmbH, Effeltrich, Germany). After incubating the samples in the dark for 20 min, maximum fluorescence (Fm) and minimum fluorescence (F0) were measured. The difference between Fm and F0 was used to compute the maximum photosynthetic quenching capacity (Fv).

2.7 *Data analysis*

Ocean Data View (ODV 5.5.1) was utilized in this study to generate site maps and environmental parameter plots. It was also employed to create spatial distribution maps for various size fractions of Chl *a*, APA, and SV. R (4.3.0) (R Core Team, 2011) was used to calculate the Pearson correlation coefficients among different parameters, construct correlation plots, and present the results of the Fv/Fm measurements and phosphate enrichment experiments. SPSS (27) (IBM Corp, 2020) was used to perform *t*-test and regression analyses.

3 Results

3.1 *Distribution of environmental factors*

Figure 2 illustrates the surface temperature, salinity, and DIP concentration distribution in the study area. The temperature decreased from 31.61℃ to 25.22℃ as the dilution of the Changjiang River plume spread outward, while the salinity increased rapidly and significantly from 0.18 to 33.32. Concurrently, the DIP concentration plummeted from 0.89 μmol/L at the CJE mouth to <0.1 μmol/L, potentially imposing phosphorus limitation for phytoplankton in the eastern study area. Furthermore, the concentration of the dissolved inorganic nitrogen at all stations surpassed 2 μmol/L.

3.2 *Distribution of Chl a*

Figure 3 depicts the surface distribution of Chl *a* in the study area. A phytoplankton bloom was observed at station B7, with micro-Chl *a*, nano-Chl *a*, and pico-Chl *a* concentrations recorded at 45.16 mg/m^3, 11.27 mg/m^3, and 8.72 mg/m^3, respectively. Apart from this station, the average micro-Chl *a*, nano-Chl *a*, and pico-Chl *a* concentrations in the surveyed area were (1.28 ±

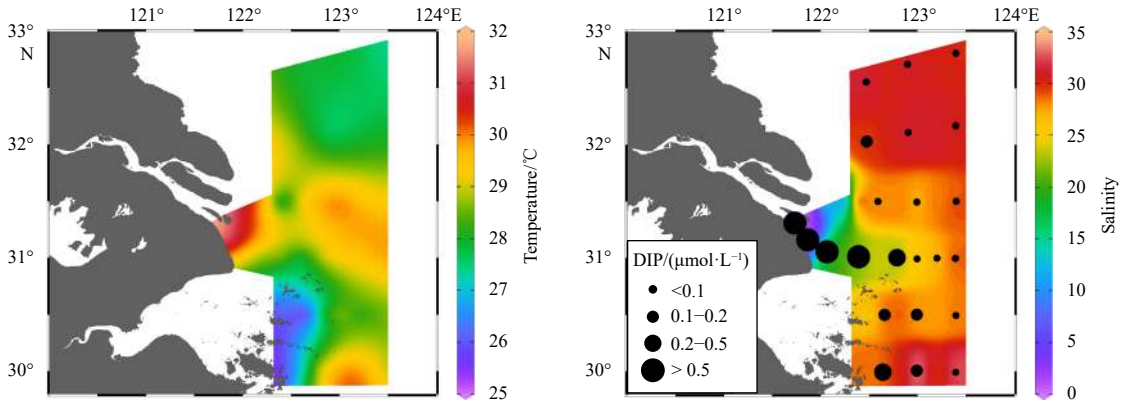

Fig. 2. Spatial distributions of sea surface temperature (a) and salinity (b) in the survey area, with black circles representing DIP concentrations.

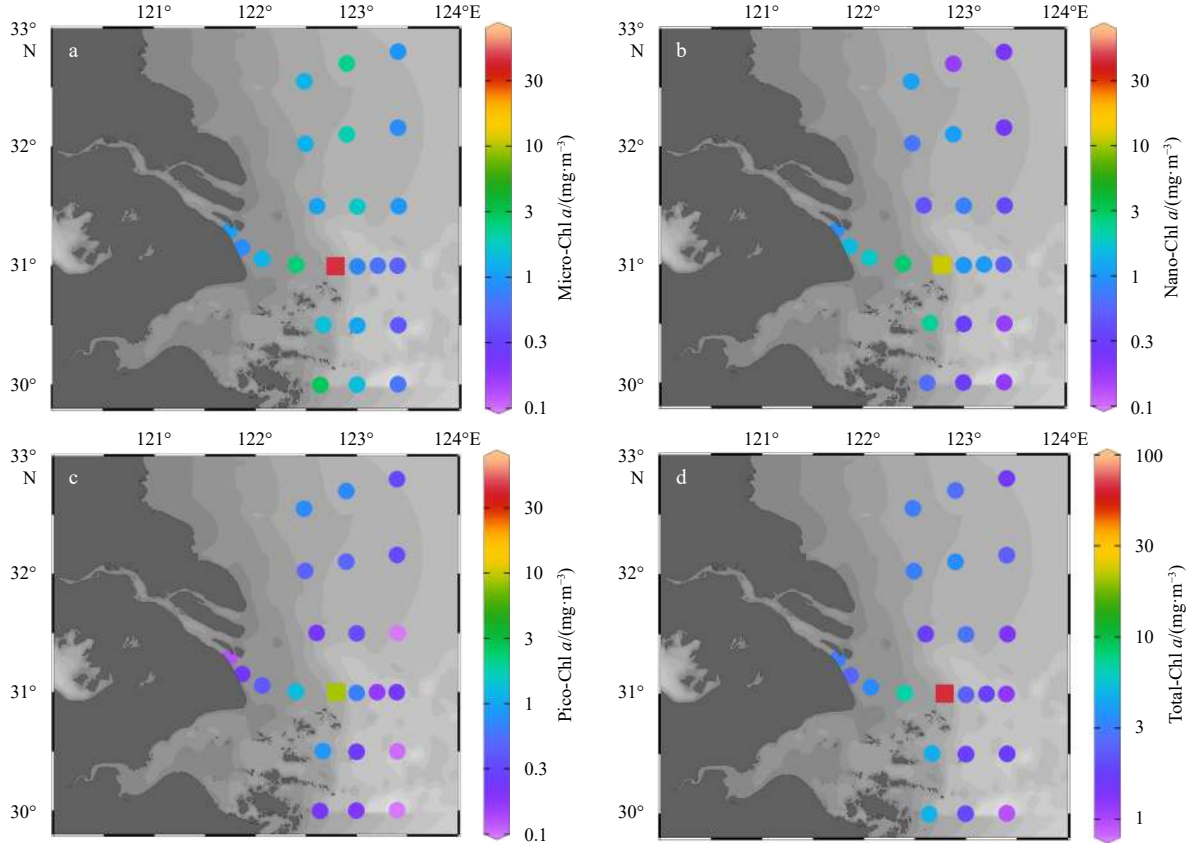

Fig. 3. Spatial distribution of surface micro- (a), nano- (b), pico- (c), and total- (d) Chl *a* concentrations in the surveyed area. Station B7 is square-marked.

0.67) mg/m^3, (0.85 ± 0.72) mg/m^3, and (0.39 ± 0.30) mg/m^3, respectively. The distribution of Chl *a* displayed a west-to-east pattern of increase followed by decrease, with higher values recorded at station B7 and its adjacent waters and lower values recorded near the CJE and the eastern part of the surveyed area (123.4°E). Across most of the study area, pico-Chl *a* concentrations consistently remained <1 mg/m^3.

3.3 *Distribution of APA*

Figure 4 depicts the spatial distribution of APA in the surveyed area. In the surveyed area, the mean concentrations of micro-, nano-, pico- and total APAs were (47.41 ± 43.56) nmol/(L·h), (33.67 ± 21.72) nmol/(L·h), (33.01 ± 33.02) nmol/(L·h), and (114.09 ± 83.81) nmol/(L·h), respectively. Lower and higher APA values were observed at the mouth of the Changjiang River and, in the northeastern region of the surveyed area and near station A5, respectively. The overall distribution of APA exhibited an increasing trend from southwest to northeast.

3.4 *Distribution of SV*

The average SV of micro-, nano-, pico-, and total-phytoplankton in the surveyed area were (1.09 ± 1.14) m/d, (0.32 ± 0.68) m/d, (–0.03 ± 0.79) m/d, and (0.65 ± 0.74) m/d, respectively, with ranges of –0.50–4.74 m/d, –1.04–1.59 m/d, –1.24–1.65 m/d, and –0.55–2.41 m/d, respectively. Figure 5 depicts the spatial distribution of these SV. High SV zones for micro- and total-phyto-

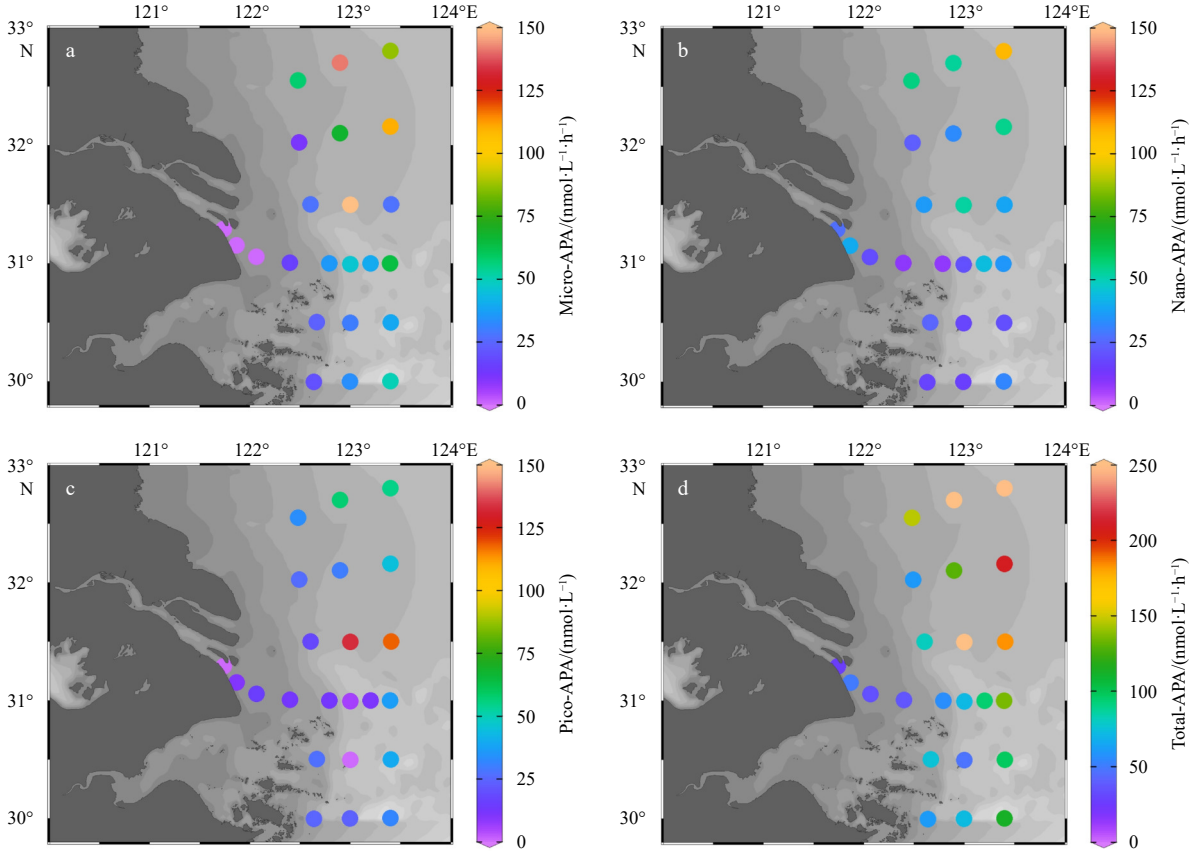

Fig. 4. Spatial distribution of surface micro- (a), nano- (b), pico- (c), and total- (d) APA concentrations in the surveyed area.

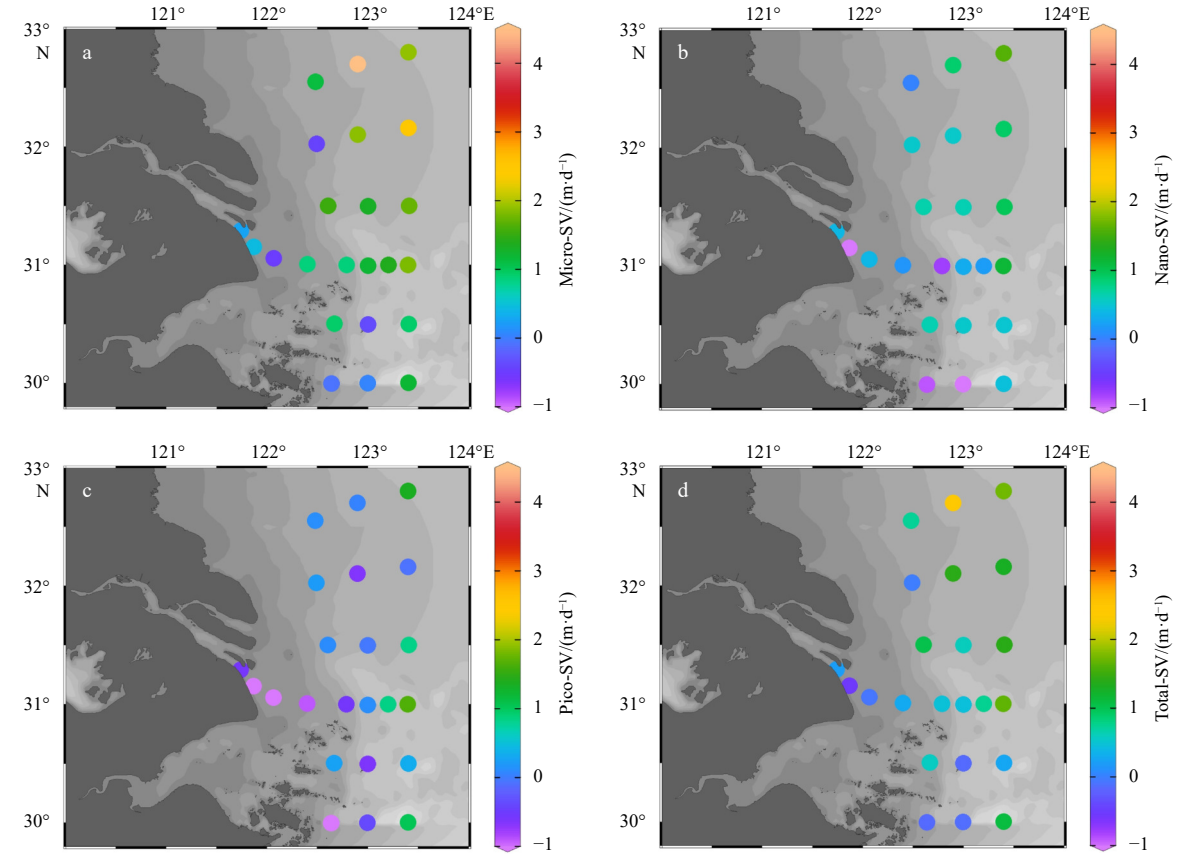

Fig. 5. Spatial distribution of surface micro- (a), nano- (b), pico- (c), and total- (d) SV in the surveyed area.

plankton were observed in the northeastern part of the surveyed area. Nano-SV increased from southwest to northeast, whereas pico-SV increased from west to east.

3.5 *Correlations between various environmental and biological parameters*

Figure 6 shows the Pearson correlation matrix for various environmental and biological parameters. In this study, most SV values across different particle size classes exhibited no statistically significant correlation with temperature. Moreover, in all particle size classes, no significant association was observed between SV or the corresponding Chl *a* concentration. However, the SVs of micro- and picophytoplankton were not significantly consistent, indicating that SV variation trends differed between phytoplankton fractions. While micro-SV was generally high (Fig. 5), the findings of this study do not suggest that a greater abundance of large-sized phytoplankton leads to higher SV. This is supported by the fact that the micro-phytoplankton proportion in the entire phytoplankton community did not exhibit a significant correlation with total-SV (not shown in Fig. 6).

Apart from that with nano-APA, the DIP concentration revealed varying degrees of statistically significant negative correlations with both APA and SV across different phytoplankton particle size categories (including total). Furthermore, for microphytoplankton, a strong and highly significant positive correlation was observed between APA and SV, whereas the correlation was attenuated slightly for nanophytoplankton. According to the regression analysis results, the impact of micro-APA on total-SV ($p = 0.042 < 0.05$) is more substantial than the influence of nano-APA on total-SV ($p = 0.096$). Therefore, the influence of microphytoplankton likely contributed to the highly significant strong positive correlation observed between total-APA and total-SV in the surveyed area.

3.6 *Relationship between Fv/Fm and total-SV*

Figure 7 depicts the relationship between Fv/Fm and the corresponding total-SV. While Pearson correlation analysis revealed no significant correlation between Fv/Fm and total SV, a significantly higher SV was observed when Fv/Fm < 0.3 (single-tailed *t*-test $p = 0.047$) than the SV at Fv/Fm > 0.3. This suggests that the relationship between the two may be nonlinear.

3.7 *The impact of phosphate enrichment on phytoplankton SV*

The SV of phytoplankton in the enrichment groups exhibited varying degrees of reduction compared to the control group. The results of the single-tailed *t*-test showed statistically significant differences in the experimental outcomes of micro-SV ($p = 0.004\,0$) and total-SV ($p = 0.001\,7$). It also exhibited statistically significant differences in nano-SV ($p = 0.039\,4$) and pico-SV ($p = 0.026\,3$).

4 Discussion

4.1 *Results comparison with other studies*

The SETCOL method (Bienfang, 1981b), known for its operational simplicity, reliable outcomes, and suitability for field experiments, has gained widespread utility (Table 1). In this study, the phytoplankton SV was determined using the SETCOL method.

In the CJE and its adjacent waters, research on summer phytoplankton SV has been conducted using the SETCOL method. Guo et al. (2016) reported results in late August, ranging from 0.28 m/d to 1.71 m/d, while Li et al. (2018) obtained results in July and September, with values range of 0.13–1.90 m/d and 0.27–3.49 m/d, respectively. The SV values of this study showed relative agreement with the values obtained from these studies.

However, they exhibited discrepancies when compared to measurements from other geographical regions, potentially at-

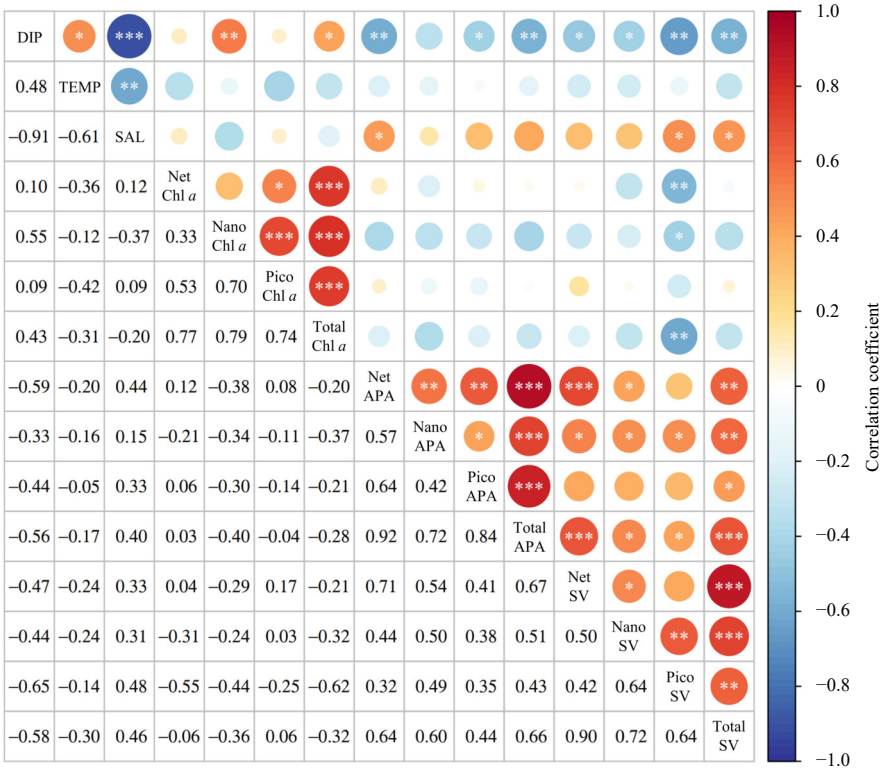

Fig. 6. Pearson correlation matrix of various environmental and biological parameters. *: $p < 0.05$; **: $p < 0.01$; ***: $p < 0.001$.

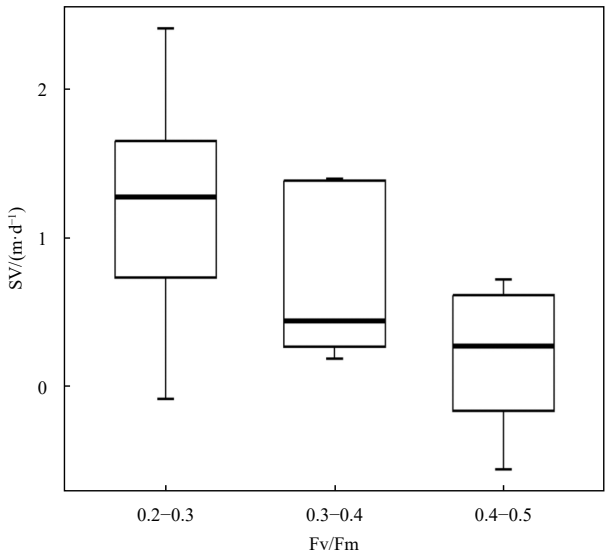

Fig. 7. Relationship between Fv/Fm and total-SV.

tributed to different variables. Pitcher et al. (1989) discovered in St. Helena Bay that micro flagellates thrive in nutrient-poor environments, whereas diatoms become the dominating community in the presence of nutrient-rich, low-oxygen upwelling, leading to an increase in SV. Nevertheless, inferring SV based solely on nutrient conditions or dominant phytoplankton species may be inaccurate. Culver and Smith (1989) found that the Greenland Sea is dominated by diatoms and dinoflagellates, with an SV ranging from –0.04 m/d to 0.63 m/d (average, 0.14 m/d), significantly lower than that in the CJE and its adjacent waters. Peperzak et al. (2003) conducted multiple measurements at the same location in the Dutch North Sea coastal zone and discovered that SV is higher when DIP and silicon (Si) concentrations are low. Therefore, conclusions drawn from diverse regions cannot be simply applied universally.

This study focuses on the CJE and its adjacent waters, where the spatial distribution of SV throughout the surveyed area exhibited discrepancies (Fig. 5). DIP concentrations were low in the northeastern region (Fig. 2b), while SV was high (Fig. 5d). The differences in their distribution and significant negative correlation (Fig. 6) indicate that the spatial variability of SV was possibly influenced by DIP distribution in the surveyed region.

4.2 *Phosphorus limitation promoted phytoplankton sinking*

The investigated area exhibited a highly significant negative correlation between surface seawater salinity and DIP concentration (Fig. 6), indicating that DIP was rapidly reduced at the front of the Changjiang River diluted seawater. According to Xu et al. (2021), the physical and chemical properties of the Changjiang River diluted water frontal zone make it a crucial "barrier" for nutrient movement, resulting in a rapid reduction of surface DIP concentrations in the Changjiang River diluted water frontal zone. Additionally, Ning et al. (2004) demonstrated that prolific phytoplankton growth could almost entirely deplete DIP in the primary productivity front of the CJE. According to these reports, the investigated area lies beyond the productivity front (Fig. 3, outskirts of station B7), with lower DIP concentrations (Fig. 2), especially in the northeastern region beyond the Changjiang River diluted waterfront, potentially imposing phosphorus limitations on phytoplankton.

Phytoplankton SV correlated negatively with DIP concentration (Fig. 6), with high SV values largely observed in the open sea (Fig. 5), particularly in regions where DIP concentrations were <0.1 μmol/L (Fig. 2), reflecting the impact of phosphorus limitation on SV. Within the investigated area, a significant positive correlation between SV and APA was observed (Fig. 6), especially in the micro-phytoplankton fraction (0.71, $p < 0.001$), suggesting that phytoplankton tended to sink more rapidly under phosphate-limited conditions. The non-linear relationship between Fv/Fm and SV indicates suboptimal physiological states in the high-SV phytoplankton, potentially because of phosphorus limitation, which could be attributed to differences in the capacity of phytoplankton of different sizes (Section 4.3) and species to cope with phosphorus limitation.

Table 1. Results of historical research on the SETCOL method

Location	SV/(m·d^{-1})	Dominant phytoplankton	Influencing factor	Reference
Friday Harbor Washington	0.96	Large and long-chained diatom	/	Bienfang and Harrison (1984)
Oligotrophic water near Oahu	0.22	Diatoms, coccolithophorids and dinoflagellates	/	Bienfang and Harrison (1984)
Resurrection Bay	0.07	Small flagellates, pennate diatoms, and coccolithophorids	N	Bienfang (1984)
Upwelling Pond (nutrient-rich water)	0.43	Large centric and pennate diatoms	N	Bienfang (1984)
Weddell Sea	0–2.73	Diatoms	Fe and Light	Johnson and Smith (1986)
Narragansett Bay	0–0.8	Diatoms	/	Riebesell (1989)
Greenland Sea	–0.04–0.63	Diatoms and dinoflagellates	N and Light	Culver and Smith (1989)
St. Helena Bay (S. Africa)	0–0.91	Flagellates and diatoms	/	Pitcher et al. (1989)
Auke Bay, Alaska	0–3.05	Chain diatoms	N	Waite et al. (1992a)
Southern Ocean	–0.5–2.4	Diatoms	Fe	Waite and Nodder (2001)
Dutch coastal zone of the North Sea	–0.4–2.2	*Phaeocystis globosa* and chain diatoms	Light, temperature, DIP, and Si	Peperzak et al. (2003)
CJE	0.13–1.71	Diatoms and dinoflagellates	Phytoplankton species	Guo et al. (2016)
CJE	0.02–3.49	Diatoms and dinoflagellates	Phytoplankton species	Li et al. (2018)
Western South China Sea	0.12–3.17	*Trichodesmium thiebautii*	Temperature and nutrients	Mao et al. (2021)
Eastern Indian Ocean	–0.29–2.19	*Trichodesmium thiebautii*	Temperature and nutrients	Wang et al. (2022a)
North-eastern South China Sea	–0.51–2.07	*Trichodesmium thiebautii*	/	Mao et al. (2023)
CJE	–0.55–2.41	Diatoms	DIP	This Study

Note: / represents no data.

Guo et al. (2016) proposed that the planktonic dinoflagellate *Prorocentrum donghaiense* Lu, characterized by active motility, exhibits greater resistance to sinking than diatoms. According to Li et al. (2018) and Mao et al. (2023), when *P. donghaiense* dominates the phytoplankton community, the SV of the planktonic flora tends to be lower. Moreover, *P. donghaiense* exhibits a significantly higher tolerance to low phosphate levels of t_p = 2.08 (Lv and Li, 2006), indicating that they can sustain a maximum growth rate for 2.08 d by utilizing stored phosphate under phosphorus limitation compared to diatoms (such as *Skeletonema costatum* with t_p = 0.53). In low-phosphate environments, dinoflagellates are more competitive (Bi et al., 2021) and die slower (Wang et al., 2006) than those in high-phosphate environments. This discrepancy in tolerance to low phosphate levels could be one of the explanations for the potential impact of the community structure on SV. Although Wang et al. (2022a) also observed higher SV in diatoms, they proposed that under optimal nutrient conditions in the environments, the phytoplankton community structure remained stable (diverse and uniform), leading to ideal cellular physiological states that were more resistant to sinking. Acuña et al. (2010) found that diatom SV approaches zero under favorable environmental conditions through an *in situ* experiment.

Many studies have used DIP concentrations that induce a rapid increase in APA levels as the threshold for phosphorus limitation. Yamaguchi (2004) determined the phosphorus limitation threshold for *S. costatum*, a dominant phytoplankton species in the CJE, to be 0.25 μmol/L (Chen et al., 2021). Similarly, Wang et al. (2022c) determined a phosphorus limitation threshold of 0.159 μmol/L for the phytoplankton community in the CJE, while Justić et al. (1995) proposed an empirical threshold of 0.1 μmol/L. Other relevant studies yielded values averaging 0.2 μmol/L (Kang et al., 2019; Zhang et al., 2018, 2021). Given that DIP concentrations at stations B8 and N6 were both <0.1 μmol/L, the phytoplankton at these locations were possibly already experiencing phosphorus limitation. The findings from the phosphate enrichment experiments (Fig. 8) indicated that compared to the SV of the control group, the phytoplankton SV in the enrichment group decreased, demonstrating statistically significant differences. Hence, it can be inferred that phosphorus limitation enhances the sinking of phytoplankton.

4.3 *SV of phytoplankton in different size fractions*

While particle size distribution did not significantly affect total-SV, larger phytoplankton may be less tolerant to phosphorus limitation. While micro-phytoplankton generally exhibited higher SV in the surveyed area (Fig. 5), the proportion of their biomass within the total-phytoplankton community did not show a significant correlation with total-SV (Section 3.5). According to Bienfang (1984), the influence of cell size on sinking is noticeable only under specific physiological conditions. In the Resurrection Bay study, Bienfang (1984) observed that during periods of ample nutrient availability in spring, the SV of micro-phytoplankton was lower than that of the total population (>0.4 μm), but it was significantly higher during the summer. This study revealed that changing environmental conditions accelerate phytoplankton community sinking beyond the Changjiang River diluted water frontal zone. Hence, micro-phytoplankton descends earlier and demonstrates a higher SV during this process than do other groups of phytoplankton, possibly owing to the reduced adaptability of larger-sized phytoplankton to phosphorus limitation. A plausible explanation is that nutrient absorption by cells results in the creation of nutrient-depleted zones on the cell surface. Owing to their low surface-to-volume ratio, efficient nutrient diffusion to larger phytoplankton cells occurs only when the surrounding environment contains a substantial concentration gradient (Karp-Boss et al., 1996).

Picophytoplankton demonstrate a tendency to resist sinking. Bienfang and Harrison (1984) proposed that this could be an innate survival strategy owing to their relatively inefficient nutrient delivery, enabling them to counteract sinking to maintain biomass. This phenomenon was reported in individual *Synechococcus* cells that exhibited difficulty in sinking (Deng et al., 2015). Similarly, Walsby (1972) demonstrated that *Cyanobacteria* that sink under high light conditions move upwards under low light circumstances, with *Microcystis* moving upward as a result of carbohydrate control (Thomas and Walsby, 1985). This may be an important area of future research, given the potential importance of small phytoplankton in carbon production (Richardson, 2018).

Notably, in certain offshore areas of the CJE, although the surface seawater exhibit low DIP concentrations, it is not the case beneath the mixed layer (Wang et al., 2009). In natural water bodies, the variations in the SV of phytoplankton, which sink due to phosphorus limitation after passing through the mixed layer, are yet to be explored. In future research, the temporal and spatial scope of observations should be broadened to gain a comprehensive understanding of the mechanisms of phytoplankton SV. Furthermore, simultaneous investigations of phytoplankton community structure would provide valuable insights.

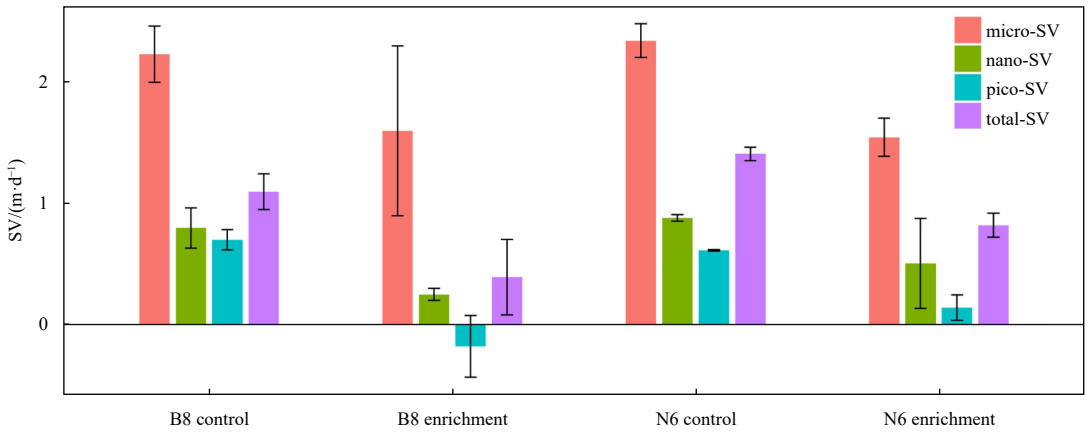

Fig. 8. Results of *in situ* phosphate enrichment experiments.

5 Conclusions

Phytoplankton plays a dual role as a fundamental component of the marine biological pump and a key contributor to hypoxia in the CJE and its adjacent waters, underscoring its substantial scientific importance. This study revealed that phosphorus limitation enhances phytoplankton SV, which could enhance our understanding of the potential mechanisms underlying hypoxic zone formation in the CJE. The key findings are summarized as follows:

(1) Considerable spatial disparities in phytoplankton SV were observed in the CJE and its adjacent waters in August. Low SV values were observed near the mouth of the Changjiang River, but higher values were observed in the northeastern region of the Changjiang River diluted waterfront. Furthermore, phytoplankton SV varied across different size fractions, with micro-phytoplankton generally exhibiting higher SV.

(2) Phytoplankton SV negatively correlated with DIP concentration and positively correlated with APA, particularly notable in micro-phytoplankton. When Fv/Fm < 0.3, a high phytoplankton SV was observed. DIP concentration regulates phytoplankton SV, with intensified phosphorus limitation resulting in higher SV, specifically influencing micro-phytoplankton sensitivity the most.

(3) The *in situ* phosphate enrichment experiments revealed that DIP supplementation led to a reduction in phytoplankton SV. Therefore, it became clear that phosphorus limitation was the primary factor driving phytoplankton sinking in the study area.

References

Acuña J L, López-Alvarez M, Nogueira E, et al. 2010. Diatom flotation at the onset of the spring phytoplankton bloom: an *in situ* experiment. Marine Ecology Progress Series, 400: 115–125, doi: 10.3354/meps08405

Ammerman J W. 1991. Role of ecto-phosphohydrolases in phosphorus regeneration in estuarine and coastal ecosystems. In: Chróst R J, ed. Microbial Enzymes in Aquatic Environments. New York: Springer

Anderson L W J, Sweeney B M. 1978. Role of inorganic ions in controlling sedimentation rate of a marine centric diatom *Ditylum brightwelli*. Journal of Phycology, 14(2): 204–214, doi: 10.1111/j.1529-8817.1978.tb02450.x

Bach L T, Stange P, Taucher J, et al. 2019. The influence of plankton community structure on sinking velocity and remineralization rate of marine aggregates. Global Biogeochemical Cycles, 33(8): 971–994, doi: 10.1029/2019GB006256

Bi Rong, Cao Zhong, Ismar-Rebitz S M H, et al. 2021. Responses of marine diatom-dinoflagellate competition to multiple environmental drivers: abundance, elemental, and biochemical aspects. Frontiers in Microbiology, 12: 731786, doi: 10.3389/fmicb.2021.731786

Bienfang P K. 1981a. Sinking rates of heterogeneous, temperate phytoplankton populations. Journal of Plankton Research, 3(2): 235–253, doi: 10.1093/plankt/3.2.235

Bienfang P K. 1981b. SETCOL — a technologically simple and reliable method for measuring phytoplankton sinking rates. Canadian Journal of Fisheries and Aquatic Sciences, 38(10): 1289–1294, doi: 10.1139/f81-173

Bienfang P K. 1984. Size structure and sedimentation of biogenic microparticulates in a subarctic ecosystem. Journal of Plankton Research, 6(6): 985–995, doi: 10.1093/plankt/6.6.985

Bienfang P K, Harrison P J. 1984. Sinking-rate response of natural assemblages of temperate and subtropical phytoplankton to nutrient depletion. Marine Biology, 83(3): 293–300, doi: 10.1007/BF00397462

Bienfang P K, Harrison P J, Quarmby L M. 1982. Sinking rate response to depletion of nitrate, phosphate and silicate in four marine diatoms. Marine Biology, 67(3): 295–302, doi: 10.1007/BF00397670

Cai Ting, Feng Yuanyuan, Xi Maonian, et al. 2022. Response of Tianjin coastal phytoplankton community to ocean acidification and nitrate enrichment. Marine Sciences (in Chinese), 46(9): 85–97

Casey J R, Mardinoglu A, Nielsen J, et al. 2016. Adaptive evolution of phosphorus metabolism in *Prochlorococcus*. mSystems, 1(6): e00065–16, doi: 10.1128/mSystems.00065-16

Chen Nansheng, Cui Zongmei, Xu Qing. 2021. Advances in the study of biodiversity of phytoplankton and red tide species in China (IV): the Changjiang Estuary. Oceanologia et Limnologia Sinica (in Chinese), 52(2): 402–417

Cloern J E. 2001. Our evolving conceptual model of the coastal eutrophication problem. Marine Ecology Progress Series, 210: 223–253, doi: 10.3354/meps210223

Correll D L. 1998. The role of phosphorus in the eutrophication of receiving waters: a review. Journal of Environmental Quality, 27(2): 261–266, doi: 10.2134/jeq1998.00472425002700020004x

Culver M E, Smith Jr W O. 1989. Effects of environmental variation on sinking rates of marine phytoplankton. Journal of Phycology, 25(2): 262–270, doi: 10.1111/j.1529-8817.1989.tb00122.x

Deng Wei, Monks L, Neuer S. 2015. Effects of clay minerals on the aggregation and subsequent settling of marine *Synechococcus*. Limnology and Oceanography, 60(3): 805–816, doi: 10.1002/lno.10059

Dyhrman S T, Jenkins B D, Rynearson T A, et al. 2012. The transcriptome and proteome of the diatom *Thalassiosira* pseudonana reveal a diverse phosphorus stress response. PLoS One, 7(3): e33768, doi: 10.1371/journal.pone.0033768

Eppley R W. 1972. Temperature and phytoplankton growth in the sea. Fishery Bulletin, 70(4): 1063–1085

Eppley R W, Holmes R W, Strickland J D H. 1967. Sinking rates of marine phytoplankton measured with a fluorometer. Journal of Experimental Marine Biology and Ecology, 1(2): 191–208, doi: 10.1016/0022-0981(67)90014-7

Falkowski P G. 2002. The ocean's invisible forest. Scientific American, 287(2): 54–61, doi: 10.1038/scientificamerican0802-54

Grasshoff K M, Kremling K, Ehrhardt M. 1976. Methods of Seawater Analysis. Weinheim: Verlag Chemie

Grosse J, Burson A, Stomp M, et al. 2017. From ecological stoichiometry to biochemical composition: variation in N and P supply alters key biosynthetic rates in marine phytoplankton. Frontiers in Microbiology, 8: 1299, doi: 10.3389/fmicb.2017.01299

Guo Shujin, Sun Jun, Zhao Qibiao, et al. 2016. Sinking rates of phytoplankton in the Changjiang (Yangtze River) Estuary: a comparative study between *Prorocentrum dentatum* and *Skeletonema dorhnii* bloom. Journal of Marine Systems, 154: 5–14, doi: 10.1016/j.jmarsys.2015.07.003

Haley S T, Alexander H, Juhl A R, et al. 2017. Transcriptional response of the harmful raphidophyte *Heterosigma akashiwo* to nitrate and phosphate stress. Harmful Algae, 68: 258–270, doi: 10.1016/j.hal.2017.07.001

Hoppe H G. 2003. Phosphatase activity in the sea. Hydrobiologia, 493(1–3): 187–200, doi: 10.1023/A:1025453918247

Huisman J, Arrayás M, Ebert U, et al. 2002. How do sinking phytoplankton species manage to persist?. The American Naturalist, 159(3): 245–254

Huisman J, Sommeijer B. 2002. Maximal sustainable sinking velocity of phytoplankton. Marine Ecology Progress Series, 244: 39–48, doi: 10.3354/meps244039

IBM Corp. 2020. IBM SPSS statistics for windows, version 27.0. Armonk, NY: IBM Corp

Johnson T O, Smith Jr W O. 1986. Sinking rates of phytoplankton assemblages in the Weddell Sea marginal ice zone. Marine Ecology Progress Series, 33: 131–137, doi: 10.3354/meps033131

Justić D, Rabalais N N, Turner R E, et al. 1995. Changes in nutrient structure of river-dominated coastal waters: stoichiometric nutrient balance and its consequences. Estuarine, Coastal and Shelf Science, 40(3): 339–356, doi: 10.1016/S0272-7714(05)80014-9

Kang Wei, Wang Zhaohui, Liu Lei, et al. 2019. Alkaline phosphatase activity in the phosphorus-limited southern Chinese coastal waters. Journal of Environmental Sciences, 86: 38–49, doi: 10.1016/j.jes.2019.04.026

Karp-Boss L, Boss E, Jumars P A. 1996. Nutrient fluxes to planktonic osmotrophs in the presence of fluid motion. Oceanography and Marine Biology, 34: 71–107

Labry C, Delmas D, Herbland A. 2005. Phytoplankton and bacterial alkaline phosphatase activities in relation to phosphate and DOP availability within the Gironde plume waters (Bay of Biscay). Journal of Experimental Marine Biology and Ecology, 318(2): 213–225, doi: 10.1016/j.jembe.2004.12.017

Li Zhao, Song Shuqun, Li Caiwen, et al. 2018. The sinking of the phytoplankton community and its contribution to seasonal hypoxia in the Changjiang (Yangtze River) Estuary and its adjacent waters. Estuarine, Coastal and Shelf Science, 208: 170–179, doi: 10.1016/j.ecss.2018.05.007

Li Hong, Veldhuis M J W, Post A F. 1998. Alkaline phosphatase activities among planktonic communities in the northern Red Sea. Marine Ecology Progress Series, 173: 107–115, doi: 10.3354/meps173107

Liu Sumei, Qi Xiaohong, Li Xiaona, et al. 2016. Nutrient dynamics from the Changjiang (Yangtze River) Estuary to the East China Sea. Journal of Marine Systems, 154: 15–27, doi: 10.1016/j.jmarsys.2015.05.010

Luo Hao, Lin Xin, Li Ling, et al. 2017. Transcriptomic and physiological analyses of the dinoflagellate *Karenia mikimotoi* reveal non-alkaline phosphatase-based molecular machinery of ATP utilisation. Environmental Microbiology, 19(11): 4506–4518, doi: 10.1111/1462-2920.13899

Lv Songhui, Li Ying. 2006. Nutritional storage ability of four harmful algae from the East China Sea. The Chinese Journal of Process Engineering (in Chinese), 6(3): 439–444

Mao Yingjie, Li Xiaoqian, Zhang Guicheng, et al. 2021. Sinking rate and community structures of autumn phytoplankton responses to mesoscale physical processes in the western South China Sea. Frontiers in Microbiology, 12: 777473, doi: 10.3389/fmicb.2021.777473

Mao Yingjie, Sun Jun, Guo Congcong, et al. 2023. Sinking rates of phytoplankton in response to cell size and carbon biomass: a case study in the northeastern South China Sea. Journal of Marine Systems, 240: 103885, doi: 10.1016/j.jmarsys.2023.103885

Mo Yu, Ou Linjian, Lin Lizhen, et al. 2020. Temporal and spatial variations of alkaline phosphatase activity related to phosphorus status of phytoplankton in the East China Sea. Science of the Total Environment, 731: 139192, doi: 10.1016/j.scitotenv.2020.139192

Muggli D L, Lecourt M, Harrison P J. 1996. Effects of iron and nitrogen source on the sinking rate, physiology and metal composition of an oceanic diatom from the subarctic Pacific. Marine Ecology Progress Series, 132(1–3): 215–227, doi: 10.3354/meps132215

Ning Xiuren, Shi Junxian, Cai Yuming, et al. 2004. Biological productivity front in the Changjiang Estuary and the Hangzhou Bay and its ecological effects. Haiyang Xuebao (in Chinese), 26(6): 96–106

Peperzak L, Colijn F, Koeman R, et al. 2003. Phytoplankton sinking rates in the Rhine region of freshwater influence. Journal of Plankton Research, 25(4): 365–383, doi: 10.1093/plankt/25.4.365

Petrucciani A, Moretti P, Ortore M G, et al. 2023. Integrative effects of morphology, silicification, and light on diatom vertical movements. Frontiers in Plant Science, 14: 1143998, doi: 10.3389/fpls.2023.1143998

Pilkaitytë R, Schoor A, Schubert H. 2004. Response of phytoplankton communities to salinity changes—a mesocosm approach. Hydrobiologia, 513(1–3): 27–38, doi: 10.1023/B:hydr.0000018162.50270.54

Pitcher G C, Walker D R, Mitchell-Lnnes B A. 1989. Phytoplankton sinking rate dynamics in the southern Benguela upwelling system. Marine Ecology Progress Series, 55(2–3): 261–269

R Core Team. 2011. R: a language and environment for statistical computing. Computing, 1: 12–21

Redfield A C, Ketchum B H, Richards F A. 1963. The influence of organisms on the composition of sea-water. In: Hill M N, ed. The Composition of Seawater: Comparative and Descriptive Oceanography. The Sea: Ideas and Observations on Progress in the Study of the Sea. New York: Interscience Publishers

Reynolds C S. 2006. The Ecology of Phytoplankton. Cambridge: Cambridge University Press

Richardson T L. 2018. Mechanisms and pathways of small-phytoplankton export from the surface ocean. Annual Review of Marine Science, 11: 57–74

Riebesell U. 1989. Comparison of sinking and sedimentation rate measurements in a diatom winter/spring bloom. Marine Ecology Progress Series, 54: 109–119, doi: 10.3354/meps054109

Smayda T J. 1970. The suspension and sinking of phytoplankton in the sea. Oceanography and Marine Biology: An Annual Review, 8: 353–414

Sun Xiaohong, Li Zhao, Ding Xueyan, et al. 2022. Effects of algal blooms on phytoplankton composition and hypoxia in coastal waters of the northern Yellow Sea, China. Frontiers in Marine Science, 9: 897418, doi: 10.3389/fmars.2022.897418

Sundareshwar P V, Morris J T, Koepfler E K, et al. 2003. Phosphorus limitation of coastal ecosystem processes. Science, 299(5606): 563–565, doi: 10.1126/science.1079100

Thomas R H, Walsby A E. 1985. Buoyancy regulation in a strain of *Microcystis*. Journal of General Microbiology, 131(4): 799–809

Tseng Y F, Lin J, Dai Minhan, et al. 2014. Joint effect of freshwater plume and coastal upwelling on phytoplankton growth off the Changjiang River. Biogeosciences, 11(2): 409–423, doi: 10.5194/bg-11-409-2014

Waite A. 1997. Sinking rate versus cell volume relationships illuminate sinking rate control mechanisms in marine diatoms. Marine Ecology Progress Series, 157: 97–108, doi: 10.3354/meps157097

Waite A, Bienfang P K, Harrison P J. 1992a. Spring bloom sedimentation in a subarctic ecosystem. I. Nutrient sensitivity. Marine Biology, 114(1): 119–129, doi: 10.1007/BF00350861

Waite A M, Nodder S D. 2001. The effect of *in situ* iron addition on the sinking rates and export flux of southern ocean diatoms. Deep-Sea Research Part II: Topical Studies in Oceanography, 48(11–12): 2635–2654, doi: 10.1016/S0967-0645(01)00012-1

Waite A M, Thompson P A, Harrison P J. 1992b. Does energy control the sinking rates of marine diatoms?. Limnology and Oceanography, 37(3): 468–477

Walsby A E. 1972. Structure and function of gas vacuoles. Bacteriological Reviews, 36(1): 1–32, doi: 10.1128/br.36.1.1-32.1972

Wang Wenliang, Chen Jianfang, Jin Haiyan, et al. 2009. The distribution characteristics and influence factors of some species phosphorus in waters of the Changjiang River Estuary in summer. Journal of Marine Sciences (in Chinese), 27(2): 32–41, doi: 10.3969/j.issn.1001-909X.2009.02.005

Wang Kui, Chen Jianfang, Jin Haiyan, et al. 2013. Nutrient structure and limitation in Changjiang River Estuary and adjacent East China Sea. Haiyang Xuebao (in Chinese), 35(3): 128–136

Wang Bin, Chen Jianfang, Jin Haiyan, et al. 2017. Diatom bloom-derived bottom water hypoxia off the Changjiang Estuary, with and without typhoon influence. Limnology and Oceanography, 62(4): 1552–1569, doi: 10.1002/lno.10517

Wang Yiheng, Hao Qiang, Chen Jianfang, et al. 2022a. Alkaline phosphatase activity of size-fractionated phytoplankton in the Changjiang Estuary in summer. Journal of Marine Sciences (in Chinese), 40(4): 25–37, doi: 10.3969/j.issn.1001-909X.2022.04.003

Wang Zongling, Li Ruixiang, Zhu Mingyuan, et al. 2006. Study on population growth processes and interspecific competition of *Prorocentrum donghaiense* and *Skeletonema costatum* in semi-continuous dilution experiments. Advances in Marine Science (in Chinese), 24(4): 495–503

Wang Xingzhou, Sun Jun, Wei Yuqiu, et al. 2022b. Response of the phytoplankton sinking rate to community structure and envir-

onmental factors in the eastern Indian Ocean. Plants, 11(12): 1534, doi: 10.3390/plants11121534

Wang Cong, Wang Jingtian, Li Ling, et al. 2022c. P-limitation promotes carbon accumulation and sinking of *Emiliania huxleyi* through transcriptomic reprogramming. Frontiers in Marine Science, 9: 860222, doi: 10.3389/fmars.2022.860222

Xu Jiajing, Zhou Peng, Lian Ergang, et al. 2021. Spatial distribution of chlorophyll *a* and its relationships with environmental factors influenced by front in the Changjiang River Estuary and its adjacent waters in summer 2019. Marine Science Bulletin (in Chinese), 40(5): 541–549

Yamaguchi H, Nishijima T, Nishitani H, et al. 2004. Organic phosphorus utilization and alkaline phosphatase production of 3 red tide phytoplankton. Nippon Suisan Gakkaishi, 70(2): 123–130, doi: 10.2331/suisan.70.123

Yang Lu, Zhang Yujia, Wang Xiaoli, et al. 2023. Spatiotemporal changes of biogenic elements in the Changjiang River Estuary and adjacent waters in summer over the last decade. Acta Oceanologica Sinica, 42(1): 83–90, doi: 10.1007/s13131-022-2104-3

Zhang Xiaohua, Lin Senjie, Liu Dongyan. 2020. Transcriptomic and physiological responses of *Skeletonema costatum* to ATP utilization. Environmental Microbiology, 22(5): 1861–1869, doi: 10.1111/1462-2920.14944

Zhang Xia, Zhang Jingping, Shen Yuan, et al. 2018. Dynamics of alkaline phosphatase activity in relation to phytoplankton and bacteria in a coastal embayment Daya Bay, South China. Marine Pollution Bulletin, 131: 736–744, doi: 10.1016/j.marpolbul.2018.05.008

Zhang Xia, Zhang Jingping, Yuan Huamao, et al. 2021. Seasonal dynamics of phytoplankton phosphorus stress in temperate Jiaozhou Bay, North China. Continental Shelf Research, 231: 104602, doi: 10.1016/j.csr.2021.104602

Zhou Feng, Chai Fei, Huang Daji, et al. 2020. Coupling and decoupling of high biomass phytoplankton production and hypoxia in a highly dynamic coastal system: the Changjiang (Yangtze River) Estuary. Frontiers in Marine Science, 7: 259, doi: 10.3389/fmars.2020.00259

Zhou Feng, Qian Zhouyi, Liu Anqi, et al. 2021. Recent progress on the studies of the physical mechanisms of hypoxia off the Changjiang (Yangtze River) Estuary. Journal of Marine Sciences (in Chinese), 39(4): 22–38

Appendix

Table A1. Results of *in situ* phosphate enrichment experiments. In the experimental group with data loss, total-SV is calculated using the remaining data

Station	Control				Enrichment			
	micro-SV/ ($m \cdot d^{-1}$)	nano-SV/ ($m \cdot d^{-1}$)	pico-SV/ ($m \cdot d^{-1}$)	total-SV/ ($m \cdot d^{-1}$)	micro-SV/ ($m \cdot d^{-1}$)	nano-SV/ ($m \cdot d^{-1}$)	pico-SV/ ($m \cdot d^{-1}$)	total-SV/ ($m \cdot d^{-1}$)
B8	1.42	0.37	–0.15	0.68	2.56	0.36	1.63	1.22
B8	2.48	0.76	1.00	1.55	2.49	/	–0.63	0.65
B8	2.09	0.75	1.49	1.50	1.84	0.23	–0.79	0.23
B8	2.88	0.41	0.84	1.21	1.07	0.31	–0.85	–0.17
B8	/	0.06	0.83	0.40	1.15	0.56	–0.73	0.20
B8	2.03	2.41	0.17	1.22	0.46	–0.28	0.27	0.20
N6	2.23	0.62	–0.48	0.96	1.07	/	0.00	0.87
N6	2.33	0.92	0.62	1.72	1.59	–0.14	–0.03	0.81
N6	2.03	1.01	1.67	1.70	1.49	0.40	0.76	1.07
N6	1.95	0.29	0.81	1.22	/	1.24	–0.45	–0.03
N6	2.27	1.20	1.83	1.94	1.32	0.82	–0.38	0.82
N6	3.21	1.22	–0.80	0.89	2.08	0.57	0.92	1.36

Note: / represents no data.